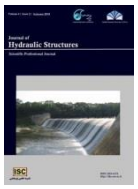
Journal of Hydraulic Structures
J. Hydraul. Struct., 2022; 8(1):1-20
DOI: 10.22055/jhs.2022.40089.1201



OPEN ACCESS

Experimental and numerical study of sluice gate flow pattern with non- suppressed sill and its effect on discharge coefficient in free-flow conditions

Rasoul Daneshfaraz [1]
Reza Norouzi [2]
Parisa Ebadzadeh[3]

Abstract

The purpose of this study is to investigate the flow pattern and discharge coefficient of sluice gate with the non-suppressed sill in experimental and numerical conditions. For this purpose, the sill of a rectangular cube in widths of 7.5, 10, 15, and 20 cm was installed under the sluice gate. Experimental results showed that placing a non-suppressed sill under the sluice gate by creating a failure in the flow lines causes a different flow pattern compared to the without sill state. Deviation of streamlines after colliding with the sill causes the formation of V-shaped currents. The discretization of equations for simulations were performed using VOF method. After selecting a cell with a size of 0.07 cm as the optimal cell, the RNG turbulence model was used. The results of the numerical simulation showed an acceptable agreement with the experimental results. Thus, the place of formation of V-shaped currents was transferred downstream of the sluice gate by increasing the width of the sill and the inflow discharge. The results of the study of the discharge coefficient showed that the placement of the sill with a width of 7.5 and 20 cm, increased the discharge coefficient by an average of 5.3% and 15.5% in the experimental model and 4.7% and 16% in the numerical simulation. This relationship is without sill state and with sill state with root mean square error of 0.967 and 0.968, respectively, estimated the discharge coefficient of the sluice gate.

Keywords: Discharge, Flow Velocity, StreamLines, Sluice Gate, Free Flow Condition

Received: 25 February 2022; Accepted: 19 March 2022

1. Introduction

The need to protect water resources and reduce water loss has led to the study of the

[1] Department of Civil Engineering, Faculty of Engineering, University of Maragheh, Maragheh, Iran, daneshfaraz@maragheh.ac.ir **(Correspond Author)**
[2] Department of Water Engineering, Faculty of Agriculture, University of Tabriz, Tabriz, Iran, rezanorouzi1992@tabrizu.ac.ir
[3] Department of Civil Engineering, Faculty of Engineering, University of Maragheh, Maragheh, Iran, ebadzadeh.p@stu.maragheh.ac.ir

performance of hydraulic structures should be considered by researchers more than before. Gates are among the hydraulic structures that control the flow, which have a special classification according to the application and location. In the meantime, the simplicity of application, the optimal accuracy of sluice gates in regulating and measuring the flow discharge has caused this structure to be considered as one of the most important water transfer structures. The most important issue in the face of sluice gates is discharge coefficient. Because by adopting functional and optimal methods, the discharge coefficient of this structure can be increased. Placing the sill under the sluice gate is one of the ways to increase the passing discharge. Previous studies have shown that embedding a sill under a sluice gate increases the discharge coefficient by altering flow characteristics such as depth and velocity.

Henry's [1] experimental study is one of the first researches in the field of sluice gates hydraulic that presented a diagram and estimated the discharge coefficient of the sluice gate. Subramania and Rajaratnam [2] studied the parameters affecting the discharge coefficient of the sluice gate experimentally. In this study, the researchers stated the direct ratio of the discharge coefficient of the sluice gate with the dimensionless *G/H* parameter. Swamee [3] described the discharge coefficient of the sluice gate as a function of the upstream water depth and the gate opening. Roth and Hager [4] by introducing anti-vortex structures, can reduced the shock waves generated downstream by 50%. In recent years, the study of factors affecting the discharge coefficient of this type of gate has attracted the attention of researchers. Ferro [5] by Using dimensional analysis and incomplete self-similarity theory, proposed a dimensionless equation for sluice gate. By combining the energy equation and the critical depth of the channel, he presented the dimensionless stage-discharge relationship. Comparison of the data obtained from the proposed relationship with the experimental results showed an acceptable agreement. Lin et al. [6] investigated the contraction coefficient of sluice gate under different hydraulic conditions. In this study, they examined the contraction coefficient of the sluice gate with a sharp-edged, circular end geometry. The contraction coefficient was estimated to be 0.59 to 0.61 for the sharp edge sluice gate and 0.65 to 0.75 for the circular sluice gate. Shivapur and Shesha Prakash [7] examined the discharge coefficient by varying the sluice gate deflection angle. In this study, four angles of 0, 15, 30, and 45 degrees were tested by deflecting the gate upwards. The results showed that the increase in gate deflection angle increases the discharge coefficient due to the increase in passing flow convergence. Akoz et al. [8] conducted experimentally and numerically to measure the velocities of 2D turbulent open channel flow upstream of a vertical sluice gate. The comparisons of the numerical and experimental results showed that the numerical simulation using the k–ε turbulence closure model predicts the velocity field and free surface profile more accurately compared to that of the k–ω turbulence model. Mohammed and Khaleel [9] studied the effect of sluice gate deflection angle on the discharge coefficient with a change in the final geometry. In this study, the deflection angle of the sluice gate in the direction of flow and the opposite direction was investigated. The results showed that a 45-degree deflection of the sluice gate in the direction of flow increases the discharge coefficient in the sluice gate with a flat end by 17.8% and by 17% in the sharp-edged gate compared to the sluice gate. Daneshfaraz et al. [10] numerically investigated the discharge coefficient of sluice gates with changes in the edge shapes. In this study, using the finite volume method, they performed simulations for sluice gate in five end geometries, including standard, jagged, rounded, sharp upward, and sharp downward.The results showed that the sluice gate with a sharp edge has the lowest discharge coefficient compared to other gates. Karami et al. [11] numerically investigated the effect of rectangular and semicircular sills on the sluice gate discharge coefficient. The team used FLOW-3D software to study the changes in sill height on the discharge coefficient. The results showed that the placement of the sill under the

sluice gate always increases the discharge coefficient. Ghorbani et al. [12] Using the H_2O method, investigated the effect of sill shape on the discharge coefficient of the sluice gate. The results of this study reported the high performance of the H_2O method in estimating the passing discharge coefficient through the sluice gate. Salmasi et al. [13] used 6 machine learning methods to study the incline sluice gate discharge coefficient. Increasing the discharge coefficient of flow by increasing the deflection angle of the sluice gate was one of the results of this study. Daneshfaraz et al. [14] investigated the different models of gate position including vertical, deflection to upstream and downstream of the channel with respect to the vertical axis and also oblique position concerning the transverse axis at angles of 10 °, 20 ° and 30 ° with FLOW-3D software. Results showed that C_d in the same discharges increases with the increasing angle to the upstream of the channel compared to the vertical position.

Examining the flow pattern in the face of the sill is one of the issues that has not been considered by researchers so far. Therefore, a study in this field is needed among researches. Because the use of sill, due to the change in the cross-section of the channel causes a change in the flow velocity characteristic. The formation of V shaped sections with different velocities distinguishes the passing flow pattern compared with the without sill state. Gate opening is one of the parameters affecting the discharge coefficient of this structure. Placing the sill under the sluice gate increases the discharge coefficient by reducing the gate opening. The importance of flow velocity is very important in the discharge coefficient of the sluice gate. Therefore, recognizing the streamlines and consequently the flow pattern created due to the presence of the sill, in addition, to safely transferring to the structure, is also effective in the discharge coefficient. In the present study, the flow pattern and discharge coefficient were studied experimentally. Then FLOW-3D software was used due to its good ability to simulate flow lines in different situations. It should be noted that a change in the width of the sill will cause a change in the parameters affecting the discharge coefficient of the sluice gate. Therefore, in this study, by introducing the effective channel width parameter in the case of using non-transverse sill, a logical comparison of the increase in discharge coefficient with the sill compared to the control mode was performed. This has not been investigated yet. Finally, a relation for estimating the discharge coefficient in the control mode and with the sill was presented.

2. Materials and methods

2.1. Dimensional analysis

The parameters affecting the discharge coefficient of the sluice gate with a sill in the free state are defined as follows (Salmasi and Norouzi [15]):

$$f_1 (C_d, \rho, Q, g, \mu, H, G, Z, b, B_1, B_2) = 0 \quad (1)$$

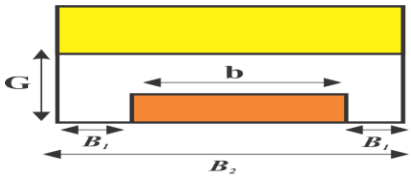


Figure 1. Cross section of sluice gate

Where C_d is the discharge coefficient (-), ρ is the water density (ML^{-3}), Q is the flow rate (L^3T^{-1}), g is the gravitational acceleration of the earth (LT^{-2}), μ is the dynamic viscosity ($ML^{-1}T^{-1}$) H is

the water depth behind the gate (L), G is the gate opening (L), Z is the sill height (L), b is the sill width (L), B_1 is the effective channel width (L) and B_2 is the laboratory flume width. According to π-Buckingham method and considering (H, g, ρ) as iterative variables, the dimensionless parameters for the gate with sill are presented as equation (2):

$$f_2\left(C_d, Fr, Re, \frac{H}{G}, \frac{H}{Z}, \frac{H}{b}, \frac{H}{B_1}, \frac{H}{B_2}\right) = 0 \quad (2)$$

In Equation (2), Fr represents the flow Froude number and Re represents the Reynolds number. Considering that 27326 < Re < 38041, the flow is turbulent and the effect of the Reynolds number is ignored. Daneshfaraz et al. [16]. The effect of the dimensionless H/Z parameter was ignored due to the constant height of the sills in all models and the channel width as a fixed parameter in all experiments was removed from the effective factors. Finally, equation (2) was rewritten as Equation (3):

$$C_d = f_3\left(\frac{H}{G}, \frac{H}{b} \cdot \frac{H}{B_1}\right) \quad (3)$$

Using dimensional analysis, dimensionless parameters H/G, H/b, and H/B_1 were extracted to investigate the passing discharge coefficient from the sluice gate. In the present study, the extracted parameters were investigated to provide a logical comparison between the silled gate and without sill state. The H/b parameter, which represents the depth of upstream water on the sill width, will have a zero denominator in the control case, which sluice gate is without sill. Also, using a non- suppressed sill will cause a change in the amount of opening in a cross-section. Therefore, the H/G dimensionless factor will not have an acceptable comparison for both state. Therefore, in the present study, by introducing the effective channel width parameter, the discharge coefficient in the gate with sill and without sill was investigated. Therefore, it can be said that the most important factor in the studies conducted in the present study is the factor H/B_1.

2.2. Experimental set-up

The experiments were performed in a laboratory flume 5 m long, 0.30 m wide, and 0.45 m high. The laboratory channel has a floor and walls made of Plexiglass and is equipped with a point depth gauge with an accuracy of ±1 mm. The inflow discharge is supplied by two pumps, each with a production capacity of 0.0083 m^3/s. A 1 cm thick sluice gate is installed one meter away from the beginning of the flume. In all experiments, the gate opening was considered constant and equal to 5 cm. The discharge applied in the present study was 700 to 1000 l/min. First, the flow pattern upstream and downstream of the sluice gate was investigated in the non-sill condition. Sills with dimensions 7.5, 10, 15, and 20 cm were installed under the sluice gate to study its effect on flow pattern and discharge coefficient. Figure (2) shows a laboratory flume schematic.

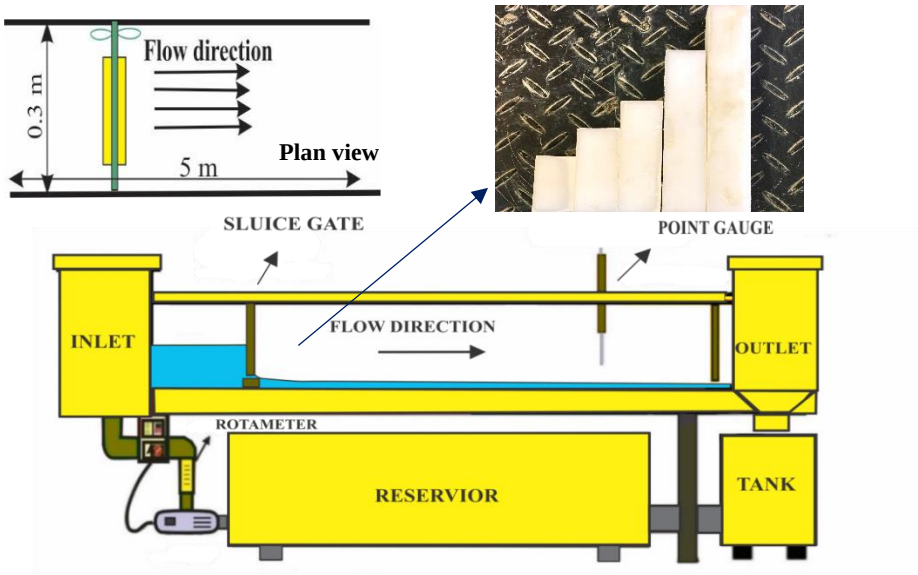


Figure 2. View of channel and sills in present study

In all experiments, after stabilizing the conditions, the flow depth was measured at three points of the channel width upstream of the sluice gate and the average depth was recorded as the final depth (H). Finally, the discharge coefficient was calculated using equation (4).

$$C_d = \frac{Q}{2A_1\sqrt{2g(H)} + A_2\sqrt{2g(H-z)}} \tag{4}$$

2.3. Flow governing equations

The simulations were performed using FLOW-3D software edition 11 version 2. This software converts partial differential equations of Navier Stokes and continuity equations by discretization method. Relations (5) to (9) express the Navier Stokes and continuity relationships, respectively.

$$\frac{\partial \rho}{\partial t} + \frac{\partial}{\partial x_i}(\rho u_i) = 0 \tag{5}$$

$$V_F\frac{\partial \rho}{\partial t} + \frac{\partial}{\partial x}(\rho u A_x) + R\frac{\partial}{\partial y}(\rho v A_y) + \frac{\partial}{\partial z}(\rho w A_z) = R_{SOR} + R_{DIF} \tag{6}$$

$$\frac{\partial u}{\partial t} + \frac{1}{V_F}\left(uA_x\frac{\partial u}{\partial x} + vA_y\frac{\partial u}{\partial y} + wA_z\frac{\partial u}{\partial z}\right) = -\frac{1}{\rho}\frac{\partial P}{\partial x} + G_x + f_x \tag{7}$$

$$\frac{\partial v}{\partial t} + \frac{1}{V_F}\left(uA_x\frac{\partial v}{\partial x} + vA_y\frac{\partial v}{\partial y} + wA_z\frac{\partial v}{\partial z}\right) = -\frac{1}{\rho}\frac{\partial P}{\partial y} + G_y + f_y \tag{8}$$

$$\frac{\partial w}{\partial t} + \frac{1}{V_F}\left(uA_x\frac{\partial w}{\partial x} + vA_y\frac{\partial w}{\partial y} + wA_z\frac{\partial w}{\partial z}\right) = -\frac{1}{\rho}\frac{\partial P}{\partial z} + G_z + f_z \tag{9}$$

In the above relations, (u, v, w) velocity components, (A_x, A_y, A_z) fraction of flow-related area, (G_x, G_y, G_z) body acceleration, (fx, f_y, f_z) viscosity acceleration in the directions (x, y, z), the R_{SOR} of the mass source, the R_{DIF} of the turbulence expression, the V_F of the volume fraction of the

fluid, and the P represent the pressure. This equation is generally expressed as relation (10).

$$\rho\left(\frac{\partial u_i}{\partial t}+u_j\frac{\partial u_i}{\partial x_i}\right)=-\frac{\partial p}{\partial x_i}+B_i+\frac{\partial}{\partial x_j}\left[\mu\left(\frac{\partial u_i}{\partial x_j}+\frac{\partial u_j}{\partial x_i}-\frac{2}{3}\delta_{ij}\frac{\partial u_k}{\partial x_k}\right)\right] \quad (10)$$

In the above relations, u_i, u_j and u_z are the components of the instantaneous velocity vector in the directions i, j, and k, respectively. *Bi* is the volumetric force in the direction i and μ of the dynamic viscosity of the fluid, ρ the specific gravity of the fluid, x_i, x_j, and x_k, respectively, represent the flow characteristics in the direction i, j and k, δ_{ij} is Kronecker delta, where if i = j, its value is equal to one, otherwise it has a value equal to zero.

2.4. Performance Metrics

To evaluate the numerical results with experimental results as well as the proposed relationship for estimating the coefficient of discharge, statistical indices of absolute error percentage (AE), relative error percentage (RE), root mean square error (RMSE), correlation coefficient (R^2) and Gupta coefficient (KGE) were used. The mentioned statistical indicators include relations 11 to 15, respectively.

$$AE=\left|C_{d_O}-C_{d_N}\right|\times 100 \quad (11)$$

$$RE=\left|\frac{C_{d_O}-C_{d_N}}{C_{d_O}}\right|\times 100 \quad (12)$$

$$RMSE=\sqrt{\frac{\sum_{i=1}^{n}(C_{d_{oi}}-C_{d_{ei}})^2}{n}} \quad (13)$$

$$KGE=1-\sqrt{(R-1)^2+(\beta-1)^2+(\gamma-1)^2} \quad (14)$$

$$R=\frac{[\sum_{i=1}^{n}(C_{d_o}-\overline{C_{d_o}})(C_{d_e}-\overline{C_{d_e}})]}{\sum_{i=1}^{n}(C_{d_o}-\overline{C_{d_o}})\sum_{i=1}^{n}(C_{d_e}-\overline{C_{d_e}})}$$

$$\beta=\frac{\overline{C_{d\,e}}}{C_{d\,o}}$$

$$=\frac{CV_e}{CV_o}=\frac{\frac{\sigma_e}{\overline{C_{d_e}}}}{\frac{\sigma_e}{\overline{C_{d_o}}}}\gamma$$

$0{,}7 < KGE < 1 \quad Very\ good$

$0{,}6 < KGE < 0{,}7 \quad Good$

$0{,}5 < KGE \leq 0{,}6 \quad Satisfactory$

$0{,}4 < KGE \leq 0{,}5 \quad Acceptable$

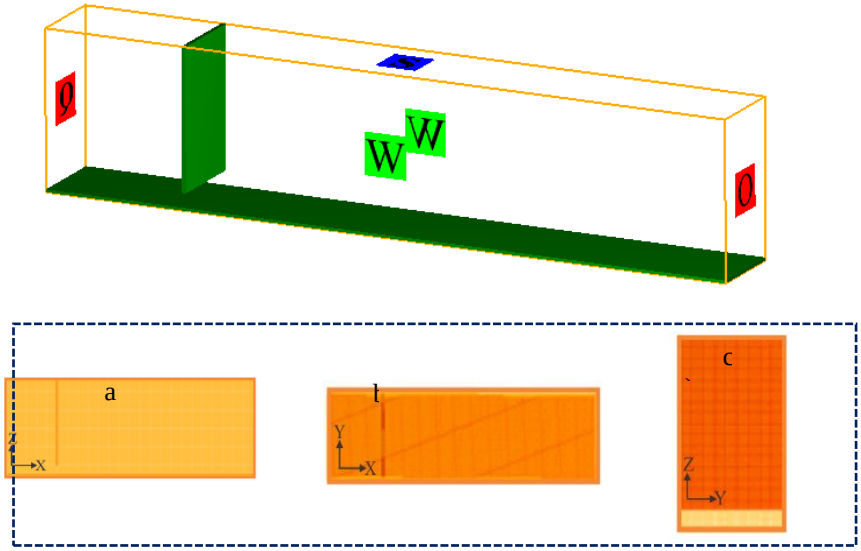
$KGE \leq 0{,}4 \quad Unsatisfactory$

In the relations of statistical indices, C_{d_o} is laboratory discharge coefficient, C_{d_N} is numerical discharge coefficient, C_{d_e} is discharge coefficient of proposed relation, $\overline{C_{d_o}}$ is average discharge coefficient of laboratory data, $\overline{C_{d_e}}$ is the mean discharge coefficient of the given relation, σ_e is the standard deviation of the data obtained from the given relation, R^2 is the correlation coefficient of the data and n represents the number of data.

2.5. Definition of the solution network and boundary conditions

To validate the numerical simulation, the laboratory data of the present study were used. First, mesh sensitivity analysis was performed by selecting the optimal mesh. Thus, with decreasing cell size, the percentage of relative error for laboratory and numerical discharge coefficient values was minimized. The values of absolute error percentage (AE) and relative error percentage (RE) were calculated with equations (11) and (12), respectively. Figure (3) shows the meshing and boundary

conditions used in the present study. The volume flow rate and output boundary conditions are used for the input and end of the channel, respectively. For the walls and floor of the channel, the boundary condition of the wall and for the upper surface, the Symmetry boundary condition is used and Figure (4) shows the comparisons of experimental and numerical simulation. Table (1) shows the characteristics and size of the cells used in this study. The RNG turbulence model was selected for the simulations due to having the lowest relative error percentage among other turbulence models. To calibrate the numerical simulation, laboratory and numerical data were examined at 5 different discharges, which are described in table (2).



ΔX = ΔY = ΔZ= 0/007 m

Figure 3. meshing and boundary conditions in this study a) X-Z direction, b) X-Y direction, c) Z-Y direction

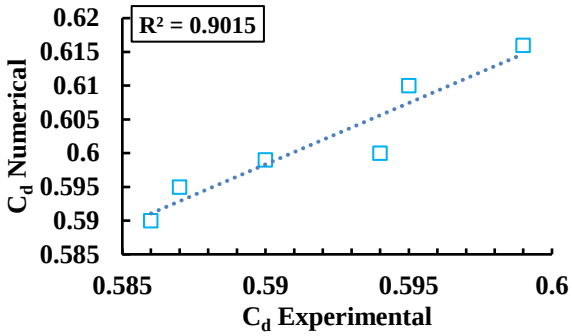


Figure. 4 Comparisons of experimental and numerical solutions

Table 1. Optimal mesh selection

Row	Cell size (cm)	Total cells	$C_{d(exp)}$	$C_{d(num)}$	AE%	RE%
1	11	312579	0.594	0.623	2.9	4.9
2	0.09	568788	0.594	0.612	1.8	3.07
3	0.08	832580	0.594	0.602	0.8	1.3
4	0.07	1228080	0.594	0.597	0.3	0.53
5	0.06	1939050	0.594	0.592	0.3	0.53

Table 2. Optimal mesh selection

ROW	Q (L/min)	$C_{d(exp)}$	$C_{d(num)}$	RE%
1	700	0.594	0.597	1.0
2	750	0.586	0.598	2.0
3	800	0.587	0.595	3.1
4	850	0.595	0.615	3.2
5	900	0.599	0.616	4.5

A total of 40 experimental models and 40 numerical simulations were investigated to study the flow pattern and its effect on the passing discharge coefficient under the sluice gate. First, the flow pattern downstream of the sluice gate without sill and with the sill was studied experimentally and numerically. Then the rate of increase of the discharge coefficient was estimated by changing the width of the sill compared to the non silled gate.

3. Results and Discussion

First, the flow pattern was examined in the non silled and with the silled gate. For this purpose, a sill with a rectangular cube geometry with widths of 7.5, 10, 15, and 20 cm was installed under the gate. First, the passing flow through the sluice gate in the state without sill was investigated. The gate opening was fixed in all experiments and was set equal to 5 cm. The inflow discharge in the control mode in the range of 0.01208 to 0.02 m^3/s was applied to the experiments. Figure (5) shows the passing flow through the sluice gate in the non silled state.

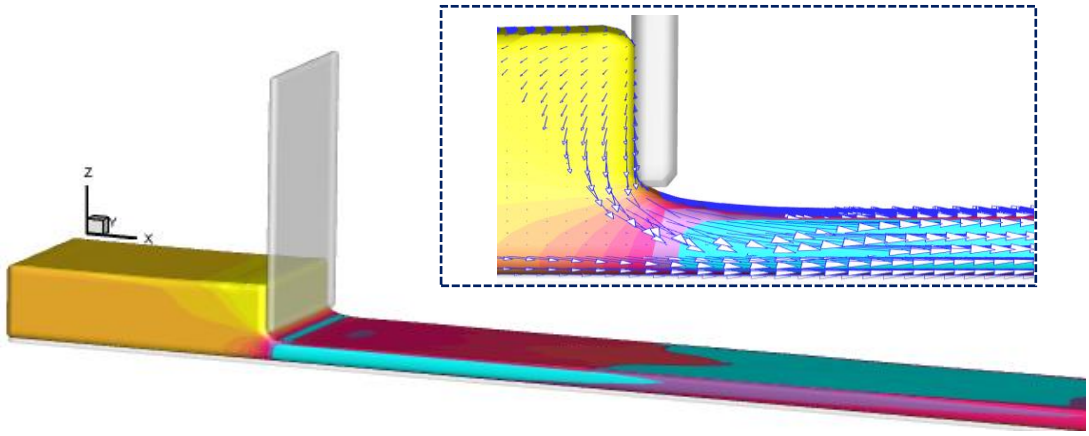


Figure 5. Flow pattern for non silled gate

Flow lines in the gate without sill, showed that upstream flow non-uniformity increases as it approaches the gate. Because the opening of the gate creates a turbulent area under the gate in which the streamlines are very irregular. Examination of the flow lines downstream of the structure showed that the supercritical current, after passing through the sluice gate, extends in parallel lines without failure. To investigate the effect of the sill on the flow pattern, a rectangular cube sill was installed under the gate. Figure (6) shows the longitudinal section of a gate with a non- suppressed sill. To clarify the streamlines, longitudinal sections a, b, and c were selected in which sections a and c are adjacent to the flume walls and have the same flow pattern, and section b represents the longitudinal section in the middle of the channel. sill placement with increasing turbulence created a different pattern for the passing fluid through the sluice gate. In this case, the increase in flow turbulence has caused the accelerating forces to be more powerful than the viscous force. As a

result, the flow behaves in an irregular pattern. The most important factor for determining the amount of flow turbulence is the ratio of inertial forces to viscosity, which is defined by the Reynolds number. As shown in Figure (6), the fluid, after passing through the sill crown, does not follow the sill shape, forming jet flows in which the fluid particles inside the flow field have different positions at each point. As a result, it causes the phenomenon of flow separation below the sill. This causes part of the streamlines to be directed upstream. The phenomenon of flow separation as well as nappe flows from the sill crown, causes the formation of a negative velocity zone. The presence of irregular velocity lines in this area is the main cause of velocity reduction in the area of flow separation in the present study.

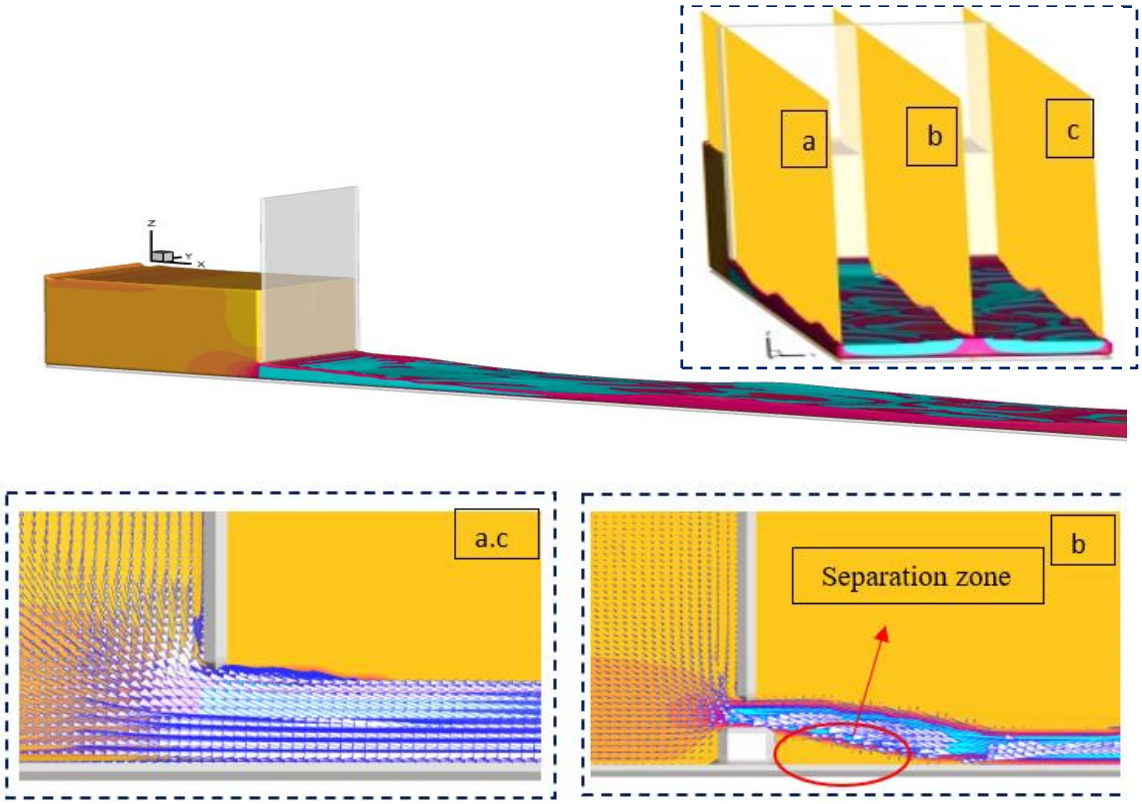


Figure 6. Flow pattern for silled gate

Examination of the upstream streamlines showed that the flow passing through the sluice gate after colliding with the sill is divided into rip flows, deflected flows, and nappe flows. The rip flows move upstream of the sill immediately after colliding the sill. These lines cause a significant energy disipation downstream of the sill. Deflected flows include lines that cross the sill sides and are transmitted downstream. The third category is the nappe flows that pass through the sill crown by creating a jet. Figures (7 a and b) show the description of the flows passing through the sluice gate with the sill experimentally and numerically, respectively.

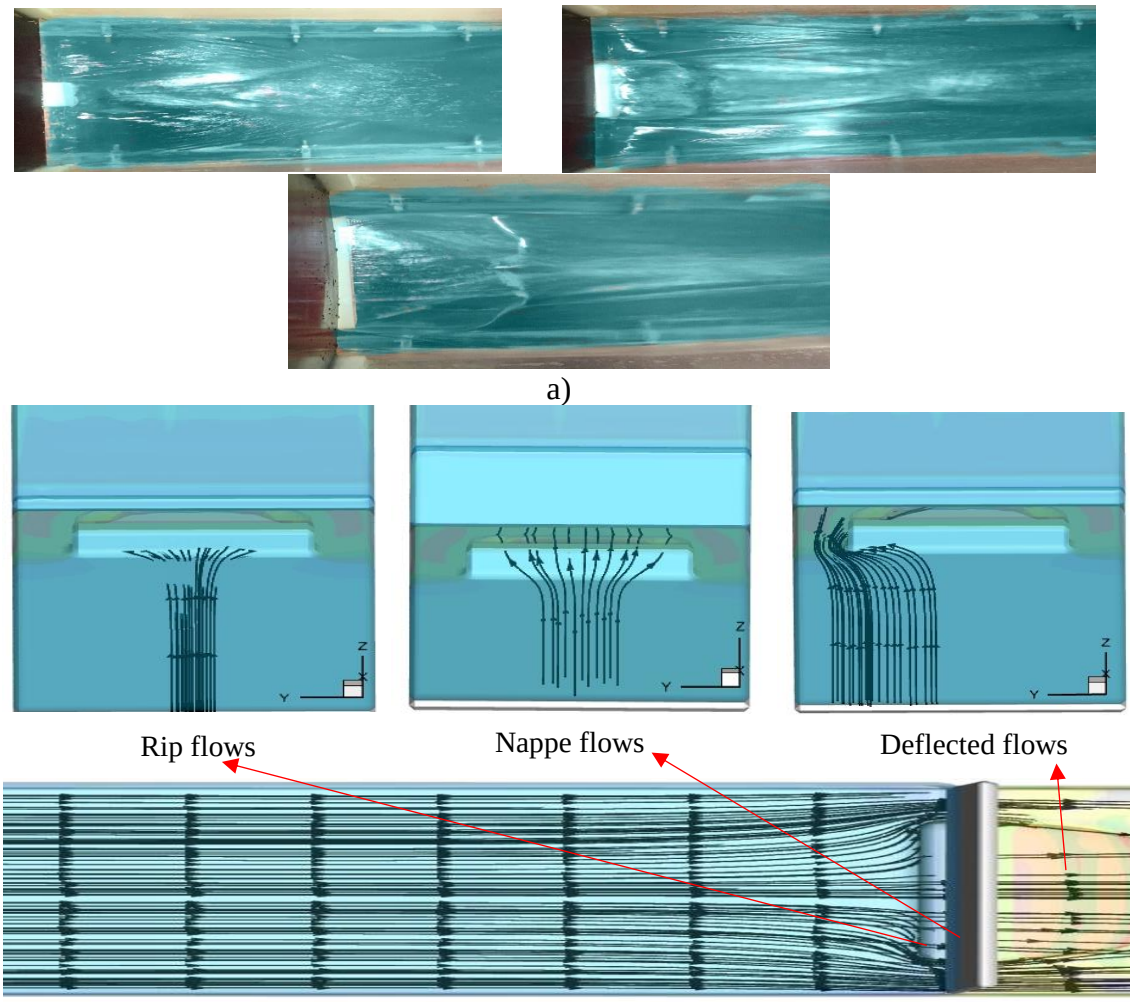


Figure 7. Flow pattern of sluice gate with sill a) Experimental views b) Numerical simulation

Nappe flows are currents that are transmitted downstream of a channel when a jet is generated. These flows appear in front of the sill due to high inertia and as a result of non-compliance of the sill shape. After flowing into the bottom of the channel, the nappe flows rise in a recurrent position, which increases the depth of water in the center of the channel relative to the vicinity of the walls. The change in the cross-section of the channel by the sill has caused the flow to diverge and failure in the flow lines after passing the vicinity of the sill by reaching a larger cross-section. The interference of nappe and deflection flows downstream of the flume has caused the formation of a V-shaped flow. Examination of streamlines showed that the deviation of flow lines to the center of the flume causes the formation of a flow separation zone adjacent to the walls, which are shown in Figure (8).

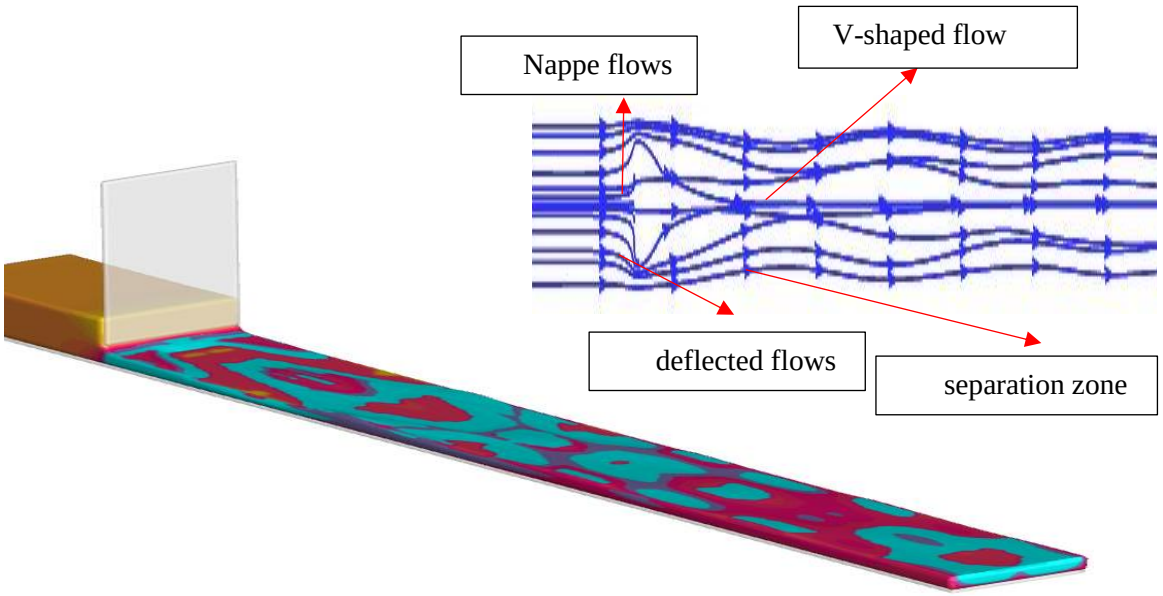
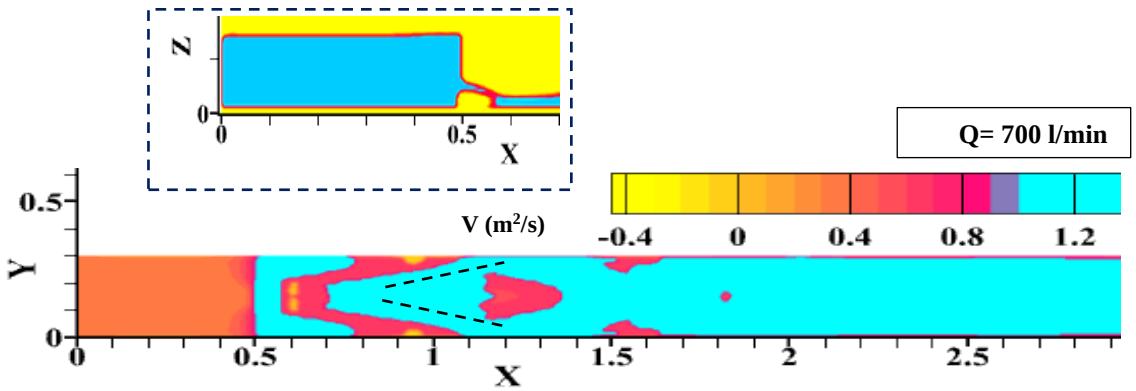


Figure 8. Simulation of flow pattern downstream of the sluice gate with the sill

Figure (8) shows the simulated flow pattern downstream of the sluice gate with the sill. The presence of nappe currents in front of the sill is another cause of the diversion of flow lines to the center of the flume. Therefore, the length of the jet resulting from the nappe currents causes a change in the intersection of the deflection and nappe currents. Therefore, increasing and decreasing the length of the jet will play an important role in the formation of the V-shaped cross-section. For this purpose, the separation areas of flow and jet length for discharges of 700, 800, and 900 l/min were investigated. Figure (9) shows the effect of inflow discharge on the flow velocity downstream of the sill and the location of the V-shaped cross-section.



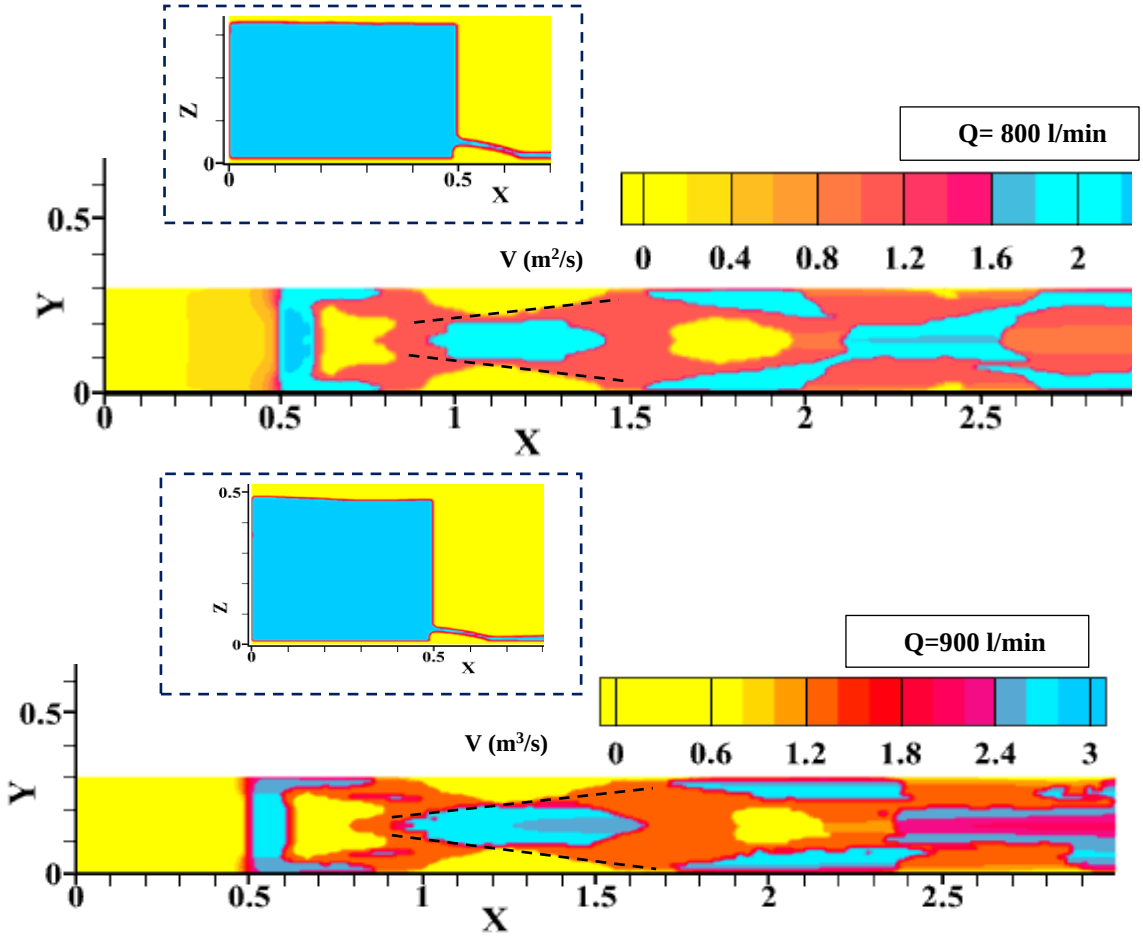


Figure 9. Flow separation zones for different discharges

X Velocity of flow is one of the important parameters in the study of hydraulic conditions of flow and hydraulic structures. Because knowing the flow velocity in different sections can reduce the damage to the structure. In Figure 9, the blue contours indicate the points with the maximum speed. Because the flow has the highest velocity when passing under the gate. The yellow contours downstream of the sluice gate are the site of the flow separation zones, which is accompanied by a decrease in velocity in this zone.In this zone, sharp changes in velocity gradient due to changes in the direction of streamlines and thus increasing shear stress cause a decrease in flow velocity. Examination of V-shaped cross-sections in different discharges showed that increasing the flow discharge intensifies the formation of this section. Thus, with the increase of discharge from 700 to 900 l/min, the length of the V-shaped cross-section has increased from 0.4 to 0.8 meters. The length of the jet was studied in different discharges. The results showed that increasing the flow velocity and consequently increasing the flow turbulence increased the non-compliance of the flow pattern with the sill shape. Figure (10) shows the longitudinal profile of the flow for jet length at different discharges.

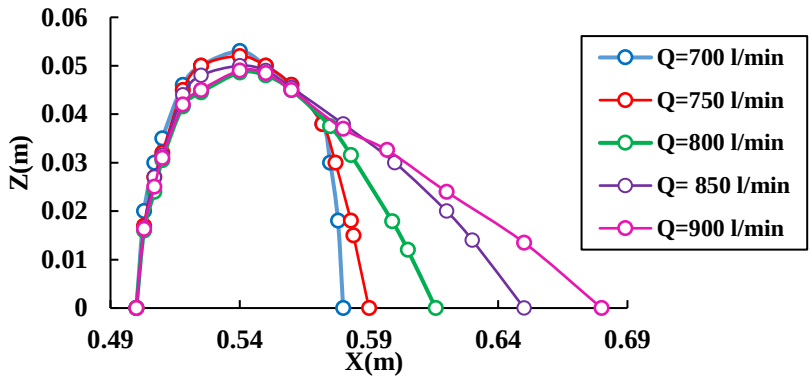
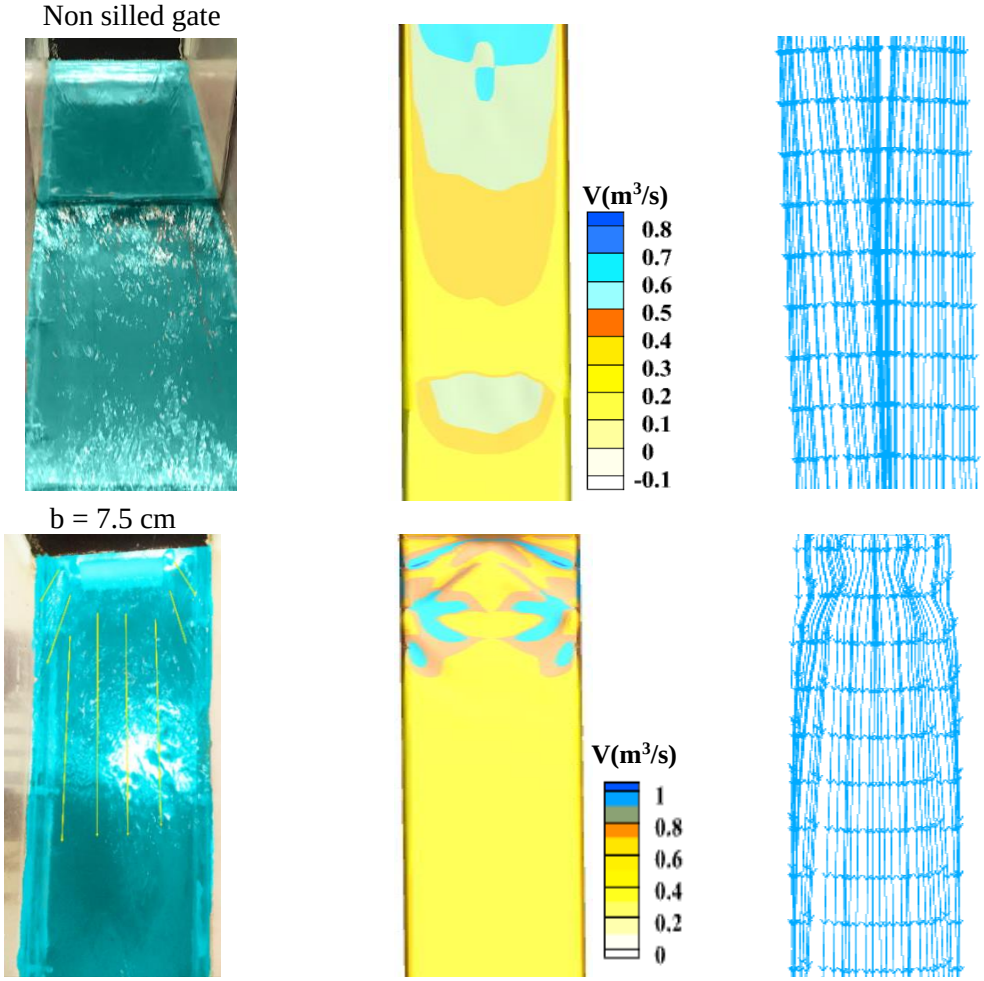


Figure 10. Longitudinal profile of the flow for jet length at different discharges

Longitudinal profile of the flow for jet length at different discharges showed that with the increase of discharge from 700 to 900 l/min, the jet length has increased to 0.1 meters. Sills with dimensions 7.5, 10, 15, and 20 cm were installed under the sluice gate to study its effect on flow pattern. Figure (11) shows the flow pattern in non silled gate compare to the sill with dimensions 7.5, 10, 15, and 20 cm.



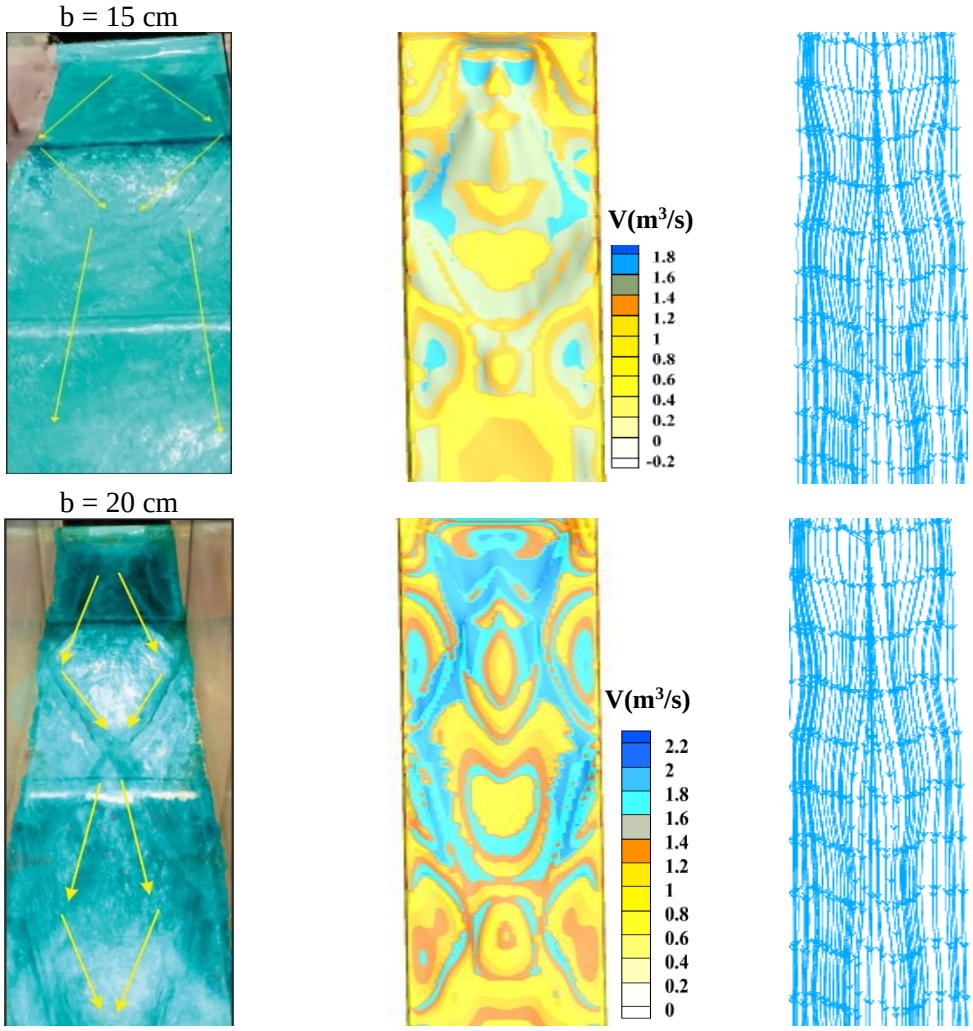


Figure 11. Flow pattern at downstream of sluice gate for non silled gate and different widths of sill

Comparison of streamlines showed that the placement of the sill affects the flow pattern downstream of the sluice gate. Examination of the flow pattern passing with a sill with a width of 7.5 cm showed that the sill with a lower width is not able to intensify the flow in the formation of a cross-section with a V-shaped flow. The numerical results obtained from the simulation of the flow pattern passing through the sluice gate indicate that the placement of the sill with a smaller width causes a slight change in the velocity of the deflecting flows in the vicinity of the sill. Therefore, the presence of low-velocity flows on both sides of the sill is not able to form a complete V-shaped flow downstream, and the current, after incompletely forming a cross-section with the V-shaped currents, extends in approximately parallel lines downstream. Sill placement, due to the difference in velocity in the cross-section of the channel, causes considerable turbulence in the sill with a larger width downstream of the gate. Nappe flows from the sill crown with a larger width are much greater than the sill state with a smaller width. On the other hand, using a sill with a larger width because it reduces the effective width of the channel in the vicinity of the walls, therefore, it increases the velocity near the walls of the flume. Comparison of velocity in the

vicinity of the sill showed that with increasing sill width, the dimensions of low-velocity zones decrease. Therefore, it can be said that the sill with a larger width increases the velocity of flow passing through the sluice gate. Due to the changes in the flow velocity, the discharge passing through the sluice gate is affected. Therefore, the discharge coefficient passing in the control mode and with the change in the sill width was examined experimentally and numerically. To study the discharge coefficient in the non silled gate state, the discharge in the range of 700 to 1000 l/min was applied to the experiments. Fixed gate opening of 5 cm was adjusted in all experiments. Figure (12) shows the discharge coefficient of the flow in the case without sill against the dimensionless parameters *H/G* and H/B_1. According to the results, it can be said that FLOW-3D software has an acceptable capability in simulating the sluice gate flow.

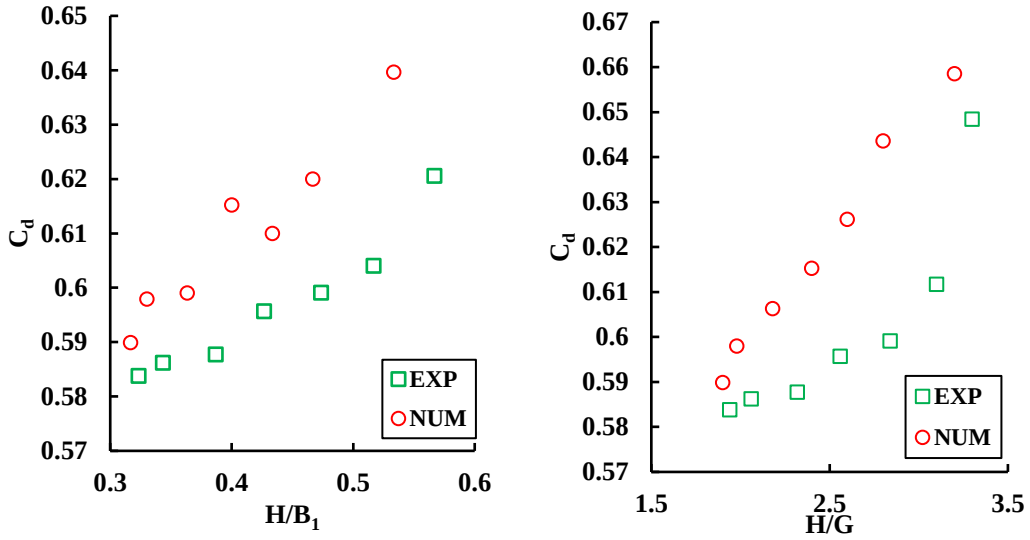


Figure 12. Comparison between experimental and numerical results of discharge coefficient for non sill state.

In Figure (12), the flow discharge coefficient has increased by increasing the two dimensionless parameters H/B_1 and *H/G*. The hydraulic reason for this is stated to be that increasing the discharge, by increasing the flow velocity, increases the discharge passing under the sluice gate. To investigate the effect of the sill on the discharge coefficient, sill with widths of 7.5, 10, 15, and 20 cm were installed under the gate. The opening of the gate was considered constant and equal to 5 cm. The height of the sills was considered to be 3 cm in all experiments. Figure (13) shows the variations of the flow discharge coefficient for the dimensionless parameter H/B_1 for the sill in different widths.

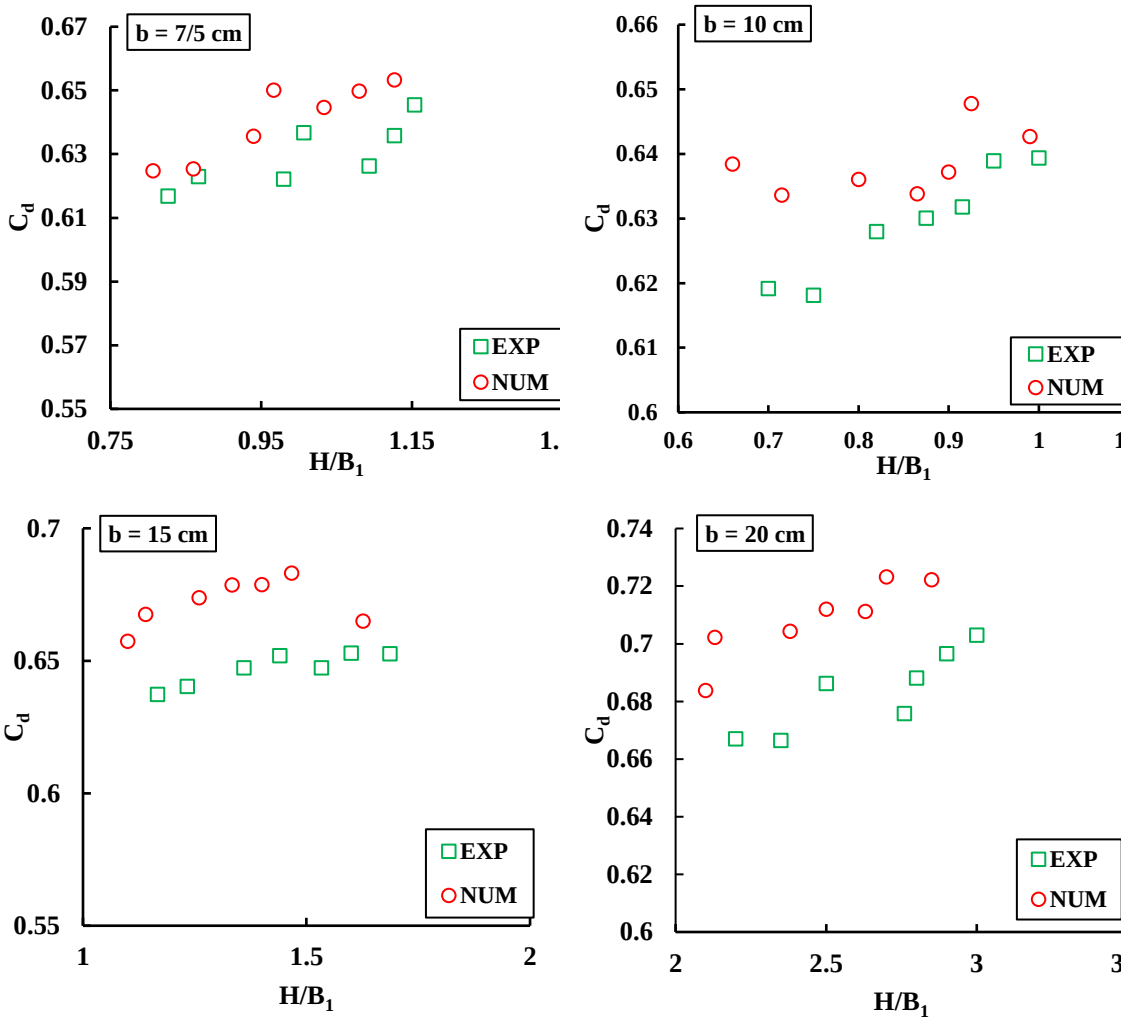


Figure 13. Comparison between experimental and numerical results of discharge coefficient for different widths of sill

The results showed that increasing the sill width causes an increase in the discharge coefficient passing through the sluice gate. The reason for this is that increasing the sill width, firstly, decreases the flow velocity by decreasing the cross-section of flow passing, and secondly, placing the sill with a larger width reduces the dimensions of the low-velocity zone in front of the sill. Therefore, placing a sill with a larger width has the highest rate of increase of the discharge coefficient. Figures (14) and (15) show the results obtained from experimental and numerical data, respectively, in the control mode and with the sill in different widths.

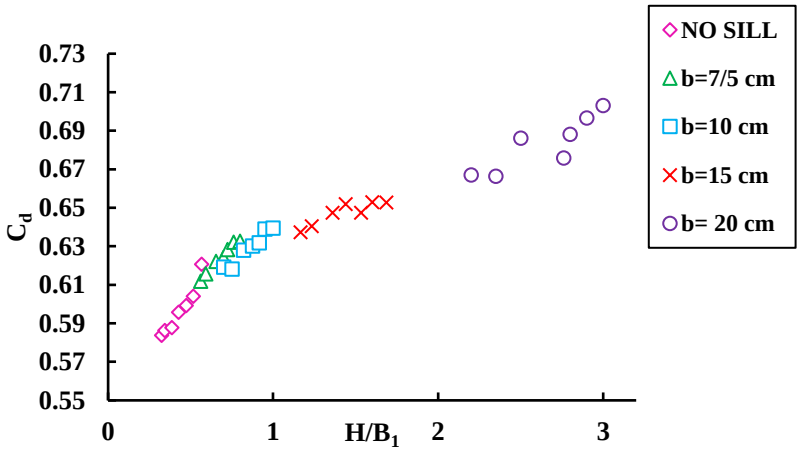


Figure 14. Experimentally Comparison between Discharge coefficient for different widths of sills and the non-sill state.

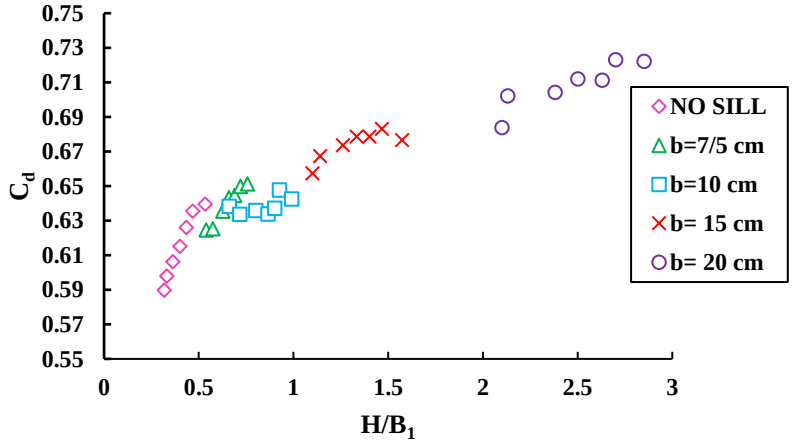


Figure 15. Numerically Comparison between Discharge coefficient for different widths of sills and the non sill state

The results showed that the placement of the sill with a width of 7.5 and 20 cm increased the discharge coefficient by an average of 5.3% and 15.5% in the laboratory mode and 4.7% and 16% in the numerical simulation compared to the mode without sill. The values of the increase of the discharge coefficient in the sill with different widths are given according to Table (3). Comparison of the flow pattern in the state with the sill showed that the larger width sill increases the discharge passing by intensifying the formation of a V-shaped cross-section indicating a high-velocity zone at the bottom as well as a decrease in the dimensions of the flow separation zone due to low velocities of flow. Therefore, it can be said that the reduction in the dimensions of the low-velocity zone, which is due to the deviation of the flow lines to the center of the channel, increases the flow velocity downstream of the sluice gate. Examination of a flow velocity as the most important characteristic affecting the discharge passing of sluice gate showed that the rate of increase of velocity downstream of the sluice gate is directly related to the discharge passing through the sluice gate. Because the placement of the sill with a larger width caused a significant increase in the value of the discharge coefficient passing.

Table 3. Increase in discharge coefficient compared to non silled gate for sills used in this study

	$b = 7{,}5\ cm$	$b = 10\ cm$	$b = 15\ cm$	$b = 20\ cm$
EXP	5.3	6.2	9.2	15.5
NUM	4.7	7.2	10.1	16.0

3.1. Estimation of discharge coefficient equations

To estimate the discharge coefficient passing through the sluice gate, the state with sill and without sill was investigated. The results showed that the discharge coefficient obtained from the simultaneous application of two dimensionless factors H/G and H/B_1 in the state without sill increased the correlation between the data. Comparison in Equations (15) to (17) indicates that Equation (17), using two dimensionless factors, the statistical index of the root mean square error in experimental and computational data is close to zero. To investigate the discharge coefficient in the state with sill, first, the effect of the dimensionless factors H/B_1 and H/b were evaluated separately in Equations (19) and (20), respectively. The results showed that the separate application of dimensional factors in estimating the discharge coefficient of the sluice gate with sill does not have acceptable accuracy. Therefore, by simultaneously applying the dimensionless parameters obtained from dimensional analysis in relation (20), the accuracy of the proposed relation was increased.

Table 4. Value of constant parameters of Equations

		a	b	c	d	KGE	RE	R^2	RMSE	Eq
$C_d = a \times (\frac{H}{G})^b$	without sill	0.001	0.96	–	–	0.90	2.22	0.89	0.004	(15)
$C_d = a \times (\frac{H}{B_1})^b$	without sill	0.005	0.87	–	–	0.89	2.4	0.85	0.007	(16)
$C_d = a \times (\frac{H}{B_1})^b + c \times (\frac{H}{G})^d$	without sill	9.6×10^{-6}	0.05	0.124	1.170	0.93	6.2	0.968	0.003	(17)
$C_d = a \times (\frac{H}{B_1})^b$	with sill	0.63	0.06	–	–	0.95	0.0003	0.938	0.006	(18)
$C_d = a \times (\frac{H}{b})^b$	with sill	0.68	0.08	–	–	0.94	1.8	0.80	0.02	(19)
$C_d = a \times (\frac{H}{B_1})^b \times c \times (\frac{H}{b})^d$	with sill	0.332	0.078	0.000028	0.036	0.93	0.15	0.967	0.004	(20)

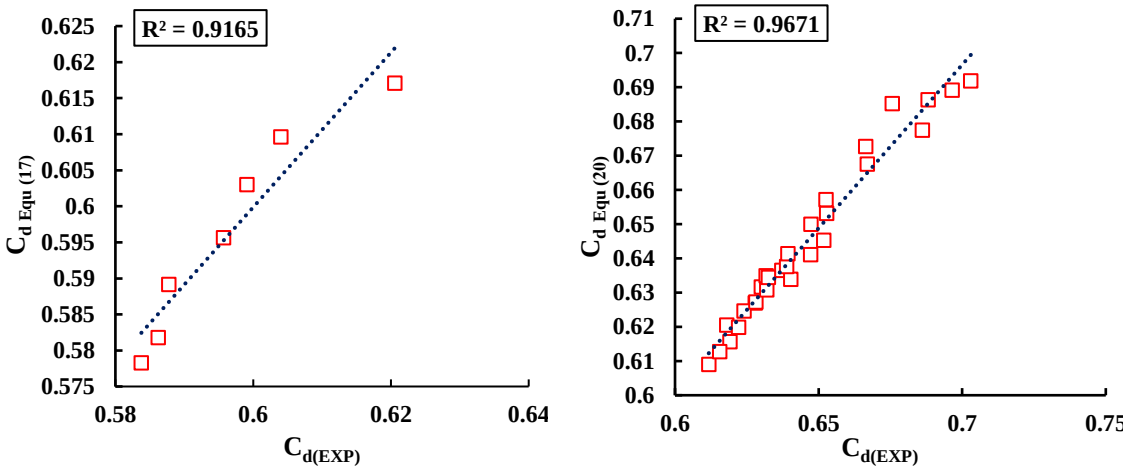


Figure 16. Correlation coefficient diagram for non silled and silled gate state

3.1. Conclusion

In the present study, the flow pattern passing of the sluice gate in the control mode with sill was investigated experimentally and numerically. The results showed that the placement of the sill under the sluice gate affects the flow pattern upstream and downstream of the sill. Examination of the flow pattern upstream the sill showed that the flow lines in the face of the sill have a specific orientation. The return lines, after colliding with the sill, cause a drop in the upstream of the sill by creating rotational currents. The nappe currents are transmitted downstream of the sill by passing through the sill crown and creating a jet. Some of the flow lines also cross the sill by deviating from their main path. Numerical studies have shown that the interference of deviant lines with the nappe currents downstream of the sill forms sections with V-shaped flows. Investigation of the location of V-shaped currents showed that the intersection of diversion and nappe flow is affected by the inflow discharge as well as the width of the sill. As the discharge and sill width increase, the location of -shaped currents progresses downstream. The reason for this is the increase in flow velocity. Because the placement of the sill with a larger width reduces the dimensions of the low-velocity separation zone. As a result, higher velocity currents are transmitted downstream. Experimental and numerical studies on the discharge coefficient showed that increasing the sill width also increases the discharge coefficient due to the increase in the flow velocity passing under the sluice gate. So that the placement of the sill with a width of 7.5 cm increased the experimental and numerical discharge coefficient of 5.3% and 4.7%, respectively. While increasing the sill width to 20 cm, the mentioned values increased to 15.5% and 16%. Comparison of the proposed relationships for estimating the discharge coefficient with the experimental data in the control mode and with sill showed that the proposed relationships have acceptable accuracy and can be used in the present study.

References

1. Henry H. R, (1950). Discussion on Diffusion of Submerged Jets, by Albertson, M. L. et al., Trans. Am. Society Civil Engrs, 115: 687.
2. Rajaratnam N, Subramanya K, (1967). Flow Equation for the Sluice Gate. Journal of the Irrigation and Drainage Division, 93(3): 167-186
3. Swamee PK, (1992). Sluice Gate Discharge Equations. Journal of Irrigation and Drainage Engineering, 118(1): 56-60.
4. Hager WH, (1999). Underflow of Standard Sluice Gate. Experiments in Fluids 27(4): 339-350. Doi: 10.1007/s003480050358.
5. Ferro V, (2000). Simultaneous flow over and under a gate. Journal of irrigation and drainage engineering 126(3): 190-193
6. Lin C.H, Yen J.F, Tsai C.T, (2002). Influence of sluice gate contraction coefficient on distinguishing condition. J. Irrigation and Drainage Eng., 128(4): 249–252
7. Shivapur. V.A, Prakash Shesha N.M, (2005). Inclined sluice gate for flow measurement. J. Hydraulic Engineering, 11(1), 46-56.
8. Akoz M, Kirkgoz M, Oner A, (2009). Experimental and Numerical Modeling of a Sluice Gate Flow. J. Hydraul. Res., 47(2): 167-176.

9. Mohammed A, Moayed K, (2013). Gate Lip Hydraulics under Sluice gate. Modern Instrumentation. 2(1): 16-19. Doi: 10.4236/mi.2013.21003.
10. Daneshfaraz R, Ghahramanzadeh A, Ghaderi A, Joudi AR, Abraham J, (2016). Investigation of the Effect of Edge Shape on Characteristics of Flow under Vertical Gates. Journal of American Water Works Association, Doi.org/10.5942/jawwa.2016.108.0102.
11. Karami S, Heidari M. M, Adib Rad M. H, (2020). Investigation of Free Flow under the Sluice Gate with the Sill Using Flow-3D Model. J. Iran Sci Technol Trans Civ Eng., 44, 317–324, Doi: 10.1007/s40996-019-0031.
12. Ghorbani M. A, Salmasi F, Saggi M. K, Norouzi R, (2020). Deep learning under H_20 framework: A novel approach for quantitative analysis of discharge coefficient in sluice gates. J. Hydroinformatics. 22(6), 1603-1619.
13. Salmasi F, Nouri M, Sihag P, Abraham J, (2021). Application of SVM, ANN, GRNN, RF, GP and RT Models For Predicting Discharge Coefficients of Oblique Sluice Gates Using Experimental Data. J. Water Supply. 21 (1): 232-248.
14. Daneshfaraz R, Abbaszadeh H, Gorbanvatan P, Abdi M, (2021). Application of Sluice Gate in Different Positions and Its Effect on Hydraulic Parameters in Free-Flow Conditions. *Journal of Hydraulic Structures*, 7(3), 72-87. doi: 10.22055/jhs.2022.39208.1196.
15. Salmasi F, Norouzi R, (2020). Investigation of different geometric shapes of sills on the discharge coefficient of a vertical sluice gate. J. Amirkabir Civil Engineering. 5(2), 1-3.
16. Daneshfaraz R, Norouzi R, Ebadzadeh P, Abbaszadeh H, (2021). Numerical investigation on effective parameters on hydraulic flows in a sluice gate with sill on free-flow condition. J. Environment and Water Engineering. doi: 10.22034/jewe.2021.295538.1596.

© 2022 by the authors. Licensee SCU, Ahvaz, Iran. This article is an open access article distributed under the terms and conditions of the Creative Commons Attribution 4.0 International (CC BY 4.0 license) (http://creativecommons.org/licenses/by/4.0/).